

# FTIR

## TALK LETTER

Vol. 38



- Development of a Boron Nitride Solid Base Catalyst and Evaluation of its Structure and Solid Basic Properties Using FTIR Spectroscopy — 02
- Using FTIR Data across Software Platforms — 06
- Good Spectra and Peak Distortion — 08
- Q&A Do All ATR Spectra Require ATR Correction? — 13
- Fourier Transform Infrared Spectrophotometer "IRXross" — 14

# Development of a Boron Nitride Solid Base Catalyst and Evaluation of its Structure and Solid Base Properties Using FTIR Spectroscopy



Department of Applied Chemistry, Faculty of Engineering, Kyushu University  
**Atsushi Takagaki**, Associate Professor

## 1. Introduction

Hexagonal boron nitride, also called white graphite, is a layered compound with a crystal structure similar to graphite. Because hexagonal boron nitride is a chemically inert and stable compound, it is often used in solid lubricants. In infrared spectroscopy, samples are frequently diluted with KBr, but boron nitride is also used to dilute samples when the X-ray absorption fine structure (XAFS) of solid powders is measured. Considering applications related to solid catalysts, boron nitride has almost exclusively been used as a catalyst support due to its chemical stability, yet recent reports show boron nitride itself also has excellent catalytic activity. A typical example of this

activity is in the oxidative dehydrogenation of light alkanes, where it was shown that boron nitride can be used as a catalyst to efficiently synthesize propylene from propane and ethylene from ethane.<sup>[1]</sup> It was also discovered that with the appropriate treatment, boron nitride can function as a high-surface-area solid base catalyst.<sup>[2]</sup> Boron nitride has demonstrated catalytic activity in the aldol reaction, nitroaldol reaction, Knoevenagel condensation, and glucose isomerization. Here an evaluation of the structure and solid basic properties of a boron nitride catalyst that was performed using infrared spectroscopy is presented.

## 2. Ball-Milled Boron Nitride Catalyst

First, highly crystalline hexagonal boron nitride was ground in a planetary ball mill.<sup>[2,3]</sup> The ball milling not only delaminated the layered structure of hexagonal boron nitride, but it also partially fragmented the boron nitride sheets and increased the surface area of the boron nitride to around  $400 \text{ m}^2\text{g}^{-1}$ . Fig. 1 shows FTIR spectra of the boron nitride before and after ball milling. Before ball milling, absorption was observed at  $1376 \text{ cm}^{-1}$  and  $819 \text{ cm}^{-1}$ , attributed to B-N stretching vibrations and B-N bending vibrations, respectively. After ball milling boron nitride at rotational speeds of at least 300 rpm, these two peaks reduced in size and several new absorption peaks appeared. Absorption at  $1079 \text{ cm}^{-1}$  and  $925 \text{ cm}^{-1}$  was attributed to B-O vibrations. Broad absorption peaks were also observed at around  $3400 \text{ cm}^{-1}$  and  $3150 \text{ cm}^{-1}$  that were attributed to O-H stretching vibrations and N-H stretching vibrations, respectively. These two absorption peaks increased in strength with increasing ball milling speed. These results show that ball milling resulted in the

formation of amino and hydroxyl groups on the solid surface of boron nitride. These functional groups on the surface are believed to have formed due to mechanical forces applied to the boron nitride during grinding and subsequent hydrolysis of the B-N backbone structure upon reaction with moisture in the air. Fig. 2 shows the relationship between ball milling speed, surface area, and the nitroaldol reaction activity. Surface area increases substantially at 300 rpm and above, the largest surface area ( $412 \text{ m}^2\text{g}^{-1}$ ) occurs at 400 rpm, and raising the ball milling speed any further reduces the surface area. This surface area reduction at higher speeds is probably due to higher surface energies at smaller particle sizes that make particles more prone to aggregation. Nitroaldol reaction activity was observed in samples after ball milling in the speed range where amino and hydroxyl groups were detected by FTIR spectroscopy (above 300 rpm), and maximum reaction activity occurred at 400 rpm.

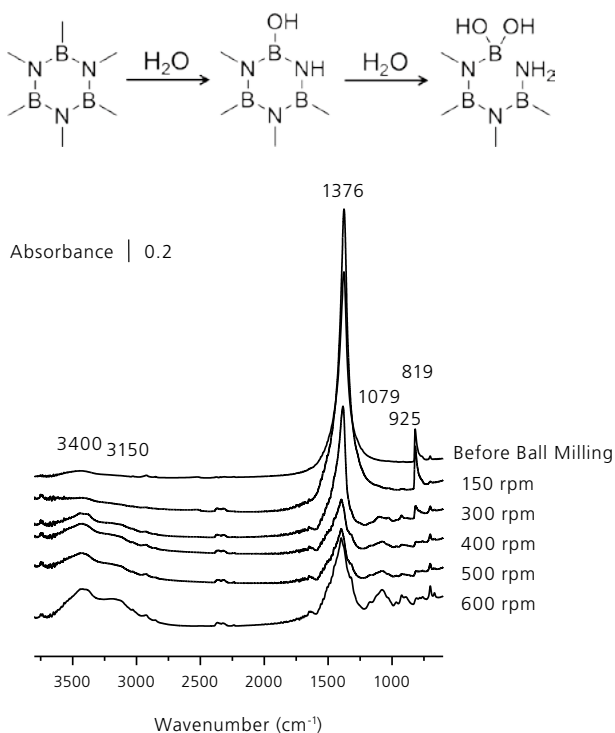


Fig. 1 FTIR Spectra of Ball-Milled Boron Nitride and Amino and Hydroxyl Group Formation

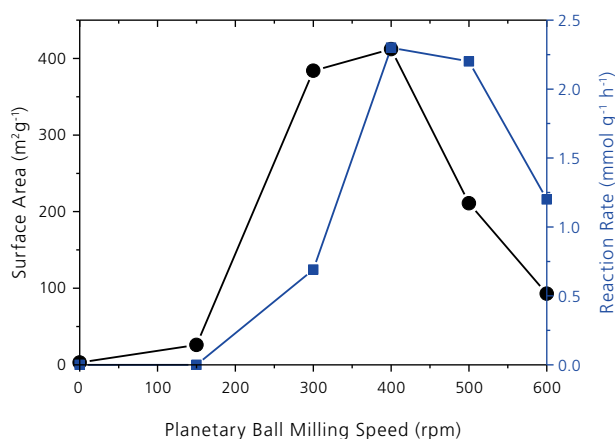


Fig. 2 Surface Area and Nitroaldol Reaction Activity of Ball-Milled Boron Nitride

### 3. Synthesizing Porous Boron Nitride Catalyst by Pyrolysis

Porous boron nitride can be synthesized from boric acid and nitrogen-containing compounds via condensation compounds by pyrolysis. Turbostratic boron nitride was synthesized by dissolving boric acid and urea in water, evaporating to dryness, transferring the resulting solid to an alumina boat, and heating at 1000 °C in an ammonia atmosphere.<sup>[4]</sup> Changing the molar ratio of boric acid and urea during synthesis from 1:2 to 1:15 (boric acid:urea) also altered the surface area and pore volume of the resulting sample significantly. A molar ratio of 1:2 synthesized boron nitride with a surface area of 376 m<sup>2</sup>g<sup>-1</sup> almost entirely derived from micropores (370 m<sup>2</sup>g<sup>-1</sup>). Using a molar ratio of 1:5, the surface area of the synthesized sample was approx. 500 m<sup>2</sup>g<sup>-1</sup> and included mesopores. This sample also contained the largest pore volume of all synthesized samples. A molar ratio of 1:10 further increased the surface area to 647 m<sup>2</sup>g<sup>-1</sup>. Synthesis by pyrolysis produced boron nitride with a higher surface area than ball milling, which only increased the surface area of boron nitride to a maximum of approx. 400 m<sup>2</sup>g<sup>-1</sup>. Fig. 3 shows the FTIR spectra of samples synthesized at different molar ratios. Similar to highly crystalline boron nitride after ball milling, the spectra show absorption by amino and hydroxyl groups. Fig. 4 presents the results obtained from a nitroaldol reaction using para-methoxy benzaldehyde and nitromethane,

and shows that catalytic activity was largely dependent on the molar ratio of boric acid and urea during synthesis. The sample synthesized at a molar ratio of 1:2 and containing only micropores shows almost no catalytic activity, and the sample synthesized at a molar ratio of 1:5 shows the highest catalytic activity with 83 % conversion. Compared with typical solid base catalysts under the same reaction conditions, the porous boron nitride showed good catalytic activity. The solid base properties of this sample were first evaluated using classical indicator reagents. Since the boron nitride samples synthesized in ammonia from boric acid and urea were white, they allowed the use of a color-changing indicator. Color development was observed on the solid sample surface with bromocresol purple (pK<sub>a</sub> = +6.3) as the indicator. No color development was observed when phenolphthalein was the indicator, showing the sample was weakly basic. Although indicator solutions are simple to use, their usefulness is limited as the target sample must be white and results could be affected by the molecular size of the indicator. The amount of solid base can also be determined by titrating with acid after color development by the indicator, but this method is often prone to error as it uses visual evaluation.

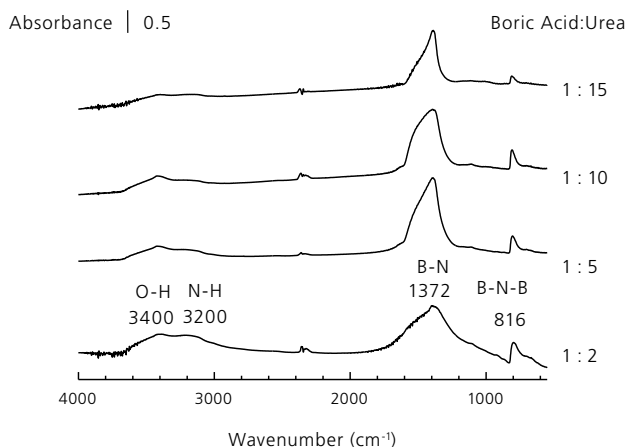


Fig. 3 FTIR Spectra of Boron Nitride Synthesized Using Boric Acid and Urea as Starting Materials

The acid-base properties of solid catalysts are often evaluated by means of FTIR spectroscopy and probe molecules. Boron nitride samples were placed in a glass IR cell and analyzed in a closed circulation system. The sample was heated under vacuum to 200 °C, then saturated deuterated chloroform ( $\text{CDCl}_3$ ) gas was adsorbed onto the sample at room temperature for 30 minutes, and after evacuating to a vacuum the FTIR spectrum was recorded. Fig. 5 shows these results as an FTIR differential spectrum of the FTIR spectra before and after adsorption. C-D stretching vibrations appear at 2252  $\text{cm}^{-1}$  due to interaction between the deuterium in chloroform and the base site of boron nitride via hydrogen bonding. According to the literature, C-D stretching vibrations appear at 2265  $\text{cm}^{-1}$  with  $\text{SiO}_2$ , 2253  $\text{cm}^{-1}$  with  $\gamma\text{-Al}_2\text{O}_3$ , and 2245  $\text{cm}^{-1}$  and 2220  $\text{cm}^{-1}$  with  $\text{MgO}$ .<sup>[5-7]</sup> By comparison with these data, the base site on synthesized boron nitride is about equivalent to  $\gamma\text{-Al}_2\text{O}_3$  but not as strongly basic as  $\text{MgO}$ .

Synthesis by pyrolysis allows selection of the starting materials. Boron nitride was synthesized by pyrolysis using the tertiary amine hexamethylenetetramine as the nitrogen-containing compound

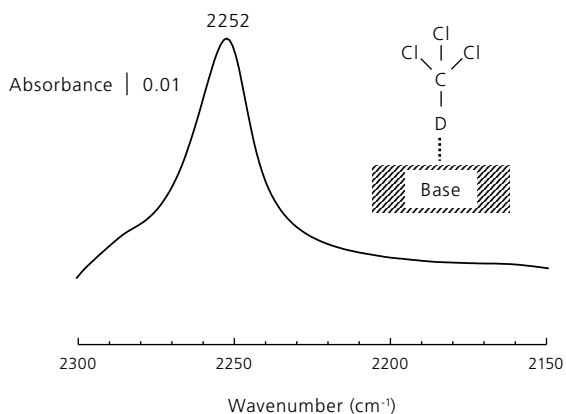


Fig. 5 FTIR Differential Spectrum of Boron Nitride (Synthesized from Boric Acid and Urea) Adsorbed with  $\text{CDCl}_3$

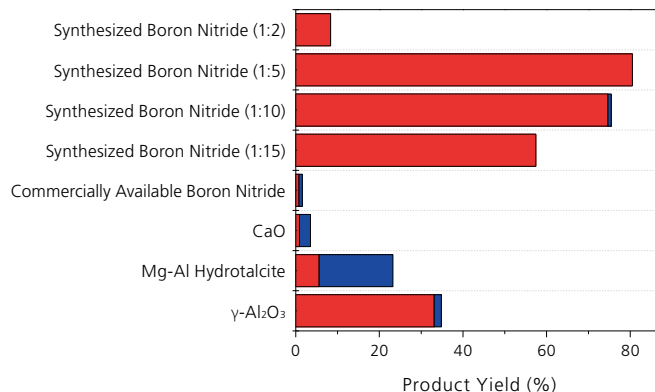
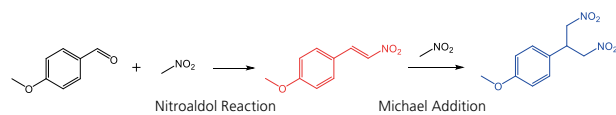


Fig. 4 Nitroaldol Reaction Using a Boron Nitride Catalyst Synthesized from Boric Acid and Urea as Starting Materials

and by mixing with boric acid.<sup>[8]</sup> Similar to the other synthesized boron nitride samples, the FTIR spectrum of this sample showed absorption at around 3400  $\text{cm}^{-1}$  derived from hydroxyl groups and at around 3200  $\text{cm}^{-1}$  derived from amine groups. The synthesized sample included oxygen in its molecular structure and was yellowish brown. Because the sample was not white, its base properties could not be evaluated with an indicator solution. Fig. 6 shows the FTIR spectrum (differential spectrum) measured after adsorbing chloroform  $\text{CHCl}_3$  as a probe molecule. Although C-H stretching vibrations appear at 3019  $\text{cm}^{-1}$  in gas phase chloroform<sup>[7]</sup>, this peak red-shifted to 2984  $\text{cm}^{-1}$  in the synthesized sample. A negative peak with its center at 3212  $\text{cm}^{-1}$  and a positive peak with its center at 3160  $\text{cm}^{-1}$  were also detected. This indicates the amino group that appears at around 3200  $\text{cm}^{-1}$  acted as a base site and interacted with the C-H of chloroform. Comparing the red-shift to 2984  $\text{cm}^{-1}$  with that of previously reported catalysts indicates that the basic strength of boron nitride synthesized with hexamethylenetetramine is stronger than that of  $\text{SiO}_2$ ,  $\gamma\text{-Al}_2\text{O}_3$ , and  $\text{NaX}$  zeolites, but weaker than that of  $\text{KX}$  and  $\text{CsX}$  zeolites.<sup>[5,9,10]</sup>

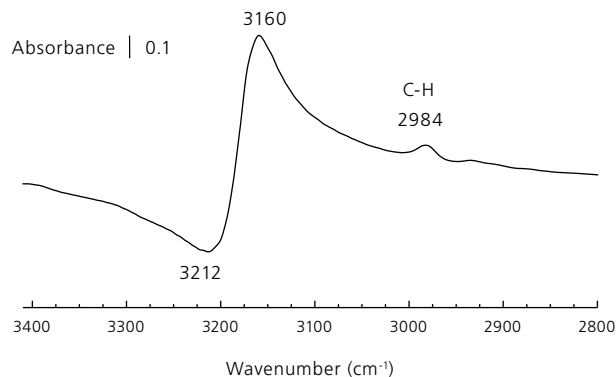


Fig. 6 FTIR Differential Spectrum of Boron Nitride (Synthesized from Boric Acid and Hexamethylenetetramine) Adsorbed with  $\text{CHCl}_3$

## 4. Conclusion

Although never previously used as a catalyst, boron nitride was found to have solid base catalytic activity when ball milled or synthesized by pyrolysis. FTIR spectroscopy was also used to evaluate the structure and solid base properties of the synthesized boron nitride. Despite being weakly basic, the synthesized boron nitride was found to be highly catalytic in base-catalyzed reactions. One of the reasons for this activity is the influence of coexisting hydroxyl groups on the surface of the solid catalyst. Experiments on substrate substituent effects suggest the nitroaldol reaction proceeds by concerted acid-base catalysis.<sup>[2-4]</sup>

When developing new catalytic materials, understanding their properties, catalytic activity, and reaction mechanisms is crucial. XPS, solid-state NMR, and soft X-ray absorption fine structure (XAFS) techniques were also used to characterize the synthesized boron nitride in addition to FTIR spectroscopy, though the details have been omitted from this article. As in the fable of the blind man and the elephant, examining a material from multiple perspectives with various measurement techniques, including FTIR spectroscopy, and grasping a complete view, provides a greater and more accurate understanding of that material.

### Acknowledgments

I would like to express my sincere appreciation to the following people who assisted in obtaining the above research findings: Shusaku Torii, Shoichiro Namba, Associate Professor Ryuji Kikuchi, Professor S. Ted Oyama (School of Engineering, The University of Tokyo (at time of writing)), Shohei Nakamura, and Professor Tatsumi Ishihara (Graduate School of Engineering, Kyushu University).

### References

- [1] J. T. Grant, C. A. Carrero, F. Goeltl, J. Venegas, P. Mueller, S. P. Burt, S. E. Specht, W. P. McDermott, A. Chiericato, I. Hermans, *Science*, **2017**, *354*, 1570-1573.
- [2] S. Torii, K. Jimura, S. Hayashi, R. Kikuchi, A. Takagaki, *J. Catal.*, **2017**, *355*, 176-184.
- [3] S. Namba, A. Takagaki, K. Jimura, S. Hayashi, R. Kikuchi, S. T. Oyama, *Catal. Sci. Technol.*, **2019**, *9*, 302-309.
- [4] S. Nakamura, A. Takagaki, M. Watanabe, K. Yamada, M. Yoshida, T. Ishihara, *ChemCatChem*, **2020**, *12*, 6033-6039.
- [5] E. P. Paukshtis, N. S. Kostsarenko, L. G. Karakchev, *React. Kinet. Catal. Lett.*, **1979**, *12*, 315-319.
- [6] P. Barteau, M.-A. Kellens, B. Delmon, *J. Chem. Soc. Faraday Trans.*, **1991**, *87*, 1425-1431.
- [7] S. Huber, H. Knözinger, *J. Mol. Catal. A*, **1999**, *141*, 117-127.
- [8] A. Takagaki, S. Nakamura, M. Watanabe, Y. Kim, J. T. Song, K. Jimura, K. Yamada, M. Yoshida, S. Hayashi, T. Ishihara, *Appl. Catal. A Gen.*, **2020**, *608*, 117843.
- [9] T. A. Gordymova, A. A. Davydov, *React. Kinet. Catal. Lett.*, **1983**, *23*, 233-238.
- [10] J. Xie, M. Huang, S. Kaliaguine, *React. Kinet. Catal. Lett.*, **1996**, *58*, 217-227.

# Using FTIR Data across Software Platforms

Spectroscopy Business Unit, Analytical & Measuring Instruments Division

Tetsuo Okuda

## 1. Introduction

Spectral data obtained by FTIR spectroscopy is used for qualitative analysis (characterizing material based on its IR spectrum) and quantitative analysis (using the height and area of specific peaks to calculate amounts of specific materials in a sample), but the data must also be prepared for analysis via various processing steps. Common data processing tasks such as ATR spectrum correction, atmospheric compensation, and operation between spectra are included as standard in analytical software provided by various companies (LabSolutions IR at Shimadzu), and because the software provided by FTIR equipment manufacturers is sufficient for typical data processing, there is usually no need to transfer data between different software products. However, in the following cases, it may be more efficient to perform data processing independently of the original software by importing that data into another software product:

- (1) To perform multiple data processing tasks
- (2) To perform the same processing task on a large amount of data
- (3) To display data in a format not available in the original FTIR control software.

To perform these types of tasks, one option is to use commercial software with advanced data processing features such as MATLAB (developed by MathWorks in the USA, a contraction of MATrix LABORatory) and another option is to use an open source process implementation system that comes with a large data processing library such as Python (a programming language created around 1990 by Guido van Rossum, a Dutch IT engineer).

Here we present directions and notes on importing FTIR spectroscopic data to perform these types of data processing tasks in other software products.

## 2. Data Export

Spectral data collected with LabSolutions IR is stored as a binary file with the extension \*.ispd (a binary file is a file composed of an arbitrary sequence of bits with no character

code convention, that is intended to be read, written, and processed by a computer program. Unlike regular text files, the contents of binary files can only be viewed by specialist software that supports the file format). Storing spectral data as a binary file has many advantages including smaller file sizes and security settings, but spectral data stored as a binary file cannot be imported by software that does not support the specific file format. LabSolutions IR includes an “Export” function that allows data to be exported in different formats for use with other software and is found in the LabSolutions IR “File” menu (see Fig. 1). To use the export function, the user opens the data to be exported, selects the desired format, and clicks “OK” to save the data in the selected file format.

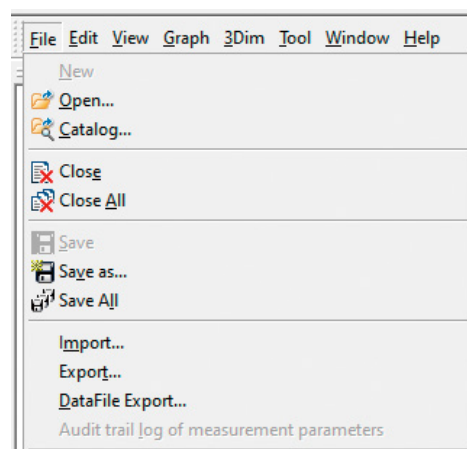


Fig. 1 File Export Function

## 3. Exportable Text-Based Data Formats and Notes on Use

The export function currently supports a variety of data formats, four of which are text-based data formats. The JCAMP-DX format was established to allow data exchange between FTIR equipment manufacturers and is an industry standard data format that is widely supported (see Fig. 2).

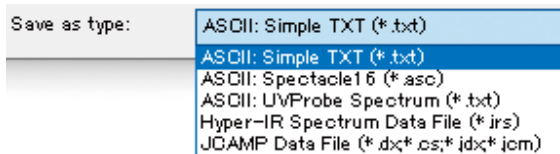


Fig. 2 Exportable File Formats

Here some features of the three exportable text-based data formats other than JCAMP-DX are explained.

### 3.1 ASCII: Simple TXT Format (\*.txt)

This format separates vertical axis values and horizontal axis values with empty spaces (see Fig. 3). When importing the data, other data processing systems use these empty spaces as delimiters.

When this data is imported by Microsoft Excel, an interactive configuration window (called a Wizard) is displayed that prompts the user to set the delimiter and identify where to separate the data.

This format contains data for both the vertical axis and horizontal axis and is simple to import and graph, but the data values are not always spaced with equal gaps because the last digit of the horizontal axis value is rounded off during export. Because of this, when data output in this format is re-imported into LabSolutions IR, the data can be displayed but data processing tasks cannot be performed on the spectrum.

```
##TITLE=Polystyrene
##DATA TYPE=INFRARED SPECTRUM
##XUNITS=1/CM
##YUNITS=%T
340.450624      182.088633
341.415073      216.244866
342.379523      248.755217
343.343972      229.285562
344.308422      357.422122
345.272871      347.696200
346.237320      344.607295
347.201770      252.318585
```

Fig. 3 Content of the Simple TXT Format (extract)

### 3.2 ASCII: Spectacle16 Format (\*.asc)

This format was supported by the HYPER-IR FTIR control software released by Shimadzu from 1996 to 2002, and has the major advantage of ensuring the gaps between data values have the same number of spaces.

The first 15 lines of this file format is a header section adapted from the JCAMP-DX format that contains the wavenumber of the first data value and last data value on the horizontal axis (##FIRSTX, ##LASTX) and the number of data points (##NPOINTS) (see Fig. 4). After this header section, the file contains only the vertical axis values in text format. Although horizontal axis values must be calculated by the user

when importing this format into another software product, this calculation step allows the user to ensure there are the same intervals between the data values. This format is considered suitable for data that will be re-imported into LabSolutions IR or will undergo data processing such as fast Fourier transform (FFT).

```
##TITLE=Polystyrene
##FORMAT=SPECTACLE-ASCII Anything
##DATA TYPE=INFRARED SPECTRUM
##SECOND TYPE=Anything
##DATE=Anything
##TIME=Anything
##SPECTROMETER/DATA SYSTEM=Anything
##XUNITS=1/CM
##YUNITS=%T
##YFACTOR=Anything
##FIRSTX=340.450624
##LASTX=4699.761731
##NPOINTS=4521.000000
##FIRSTY=Anything
##XYDATA=( Y..Y )
182.088633
216.244866
248.755217
229.285562
```

Fig. 4 Content of the Spectacle16 Format (extract)

### 3.3 ASCII: UVProbe Spectrum Format (\*.txt)

UVProbe is the control software for Shimadzu's UV-Vis spectrophotometers and UVProbe Spectrum is the format used to import data into UVProbe. The files contain comma-separated text (normally associated with the .csv extension), so the UVProbe Spectrum format is useful for importing into Microsoft Excel. However, because this format uses the .txt extension and not .csv, the following steps must be performed.

- (1) Create a working folder and copy the file(s) to be converted into the working folder.
- (2) Using a suitable text editor, enter the following and save in the working folder with the name "RenTXT2CSV.bat."

```
Ren *.txt *.csv
```

- (3) In Explorer, double-click on the RenTXT2CSV.bat file.

Performing the above steps (1) to (3) will save all data files in the working folder with the .csv extension.

## 4. Conclusion

This article explained the text file formats that can be exported using LabSolutions IR. We hope you will utilize these file formats when considering data processing across software platforms.

# Good Spectra and Peak Distortion

Solutions COE, Analytical & Measuring Instruments Division

Yasushi Suzuki

What does the phrase “good spectrum” mean when measuring spectra with an FTIR spectrophotometer? Which spectrum is required depends on its intended use, and spectra can be evaluated based on various indicators. This article explains the causes of peak distortion while also explaining how to obtain a good spectrum.

## 1. What is a Good Spectrum?

Good spectra that show transmittance are determined based on baseline, peak intensity, and peak shape.

### (1) “A Horizontal Baseline that Does Not Exceed 100 %”

The first factor to consider is whether the baseline is horizontal.

For transmission spectra, the baseline is sometimes lower at high wavenumbers and higher at low wavenumbers, i.e., the baseline of a spectrum showing transmittance rises up to the right. This is probably caused by scattering at the sample.

For ATR spectra, the baseline can slope in the opposite direction, i.e., the baseline is higher at high wavenumbers and lower at low wavenumbers. For samples such as rubber that contain a large amount of carbon, sloping may indicate absorption by carbon across the entire wavenumber range. Specifically, light penetrates deeper at lower wavenumbers during ATR spectroscopy, hence carbon absorption is stronger at lower wavenumbers, causing the baseline of a spectrum showing transmittance to fall away to the right.

The next factor to consider is the position of the baseline. A spectrum baseline may not exceed 100 % in theory, but in practice, some spectrum baselines exceed 100 %. When using the KBr pellet method, baselines can exceed 100 % when the background pellet is cloudy and the sample pellet is transparent and the sample pellet is more transmissive than the background pellet.

### (2) “The Strongest Peak Intensity is No Less Than 5 %”

During transmission measurements, the strongest peak intensity may fall below 5 % transmittance when the sample is thick or highly concentrated. In such cases, the sample must be modified such as by making the sample thinner or more dilute.

The Japanese Pharmacopoeia states “prepare [the specimen] so that the transmittance of most of the absorption bands is in the range of 5 % to 80 %,” while the Japanese Industrial Standard (JIS) General Rules for Infrared Spectrophotometric Analysis (K 0117:2017) states “concentration should be adjusted so that the transmittance of the strongest absorption band is at least 5 %.”

In special cases when the strongest peak intensity is below 5 % transmittance, minor peaks may be of interest. In such cases, strong peaks are saturated intentionally to ensure minor peaks of interest are clearly visible.



## 2. Peak Distortion and Good Spectra

### (1) Refractive Index

Absorption peaks are often almost symmetrical, though strong absorption peaks may show broadening on the low wavenumber side. Accordingly, whether a peak shape is symmetrical or not is related to the strength of the absorption peak.

But why does a strong absorption peak become asymmetric? The refractive index of samples is known to vary across the wavenumber range of a given peak.

Fig. 1 shows an absorption peak where the refractive index  $n_2$  and absorption coefficient  $k$  vary on either side of the peak, and  $\nu_0$  is the position of the absorption peak.

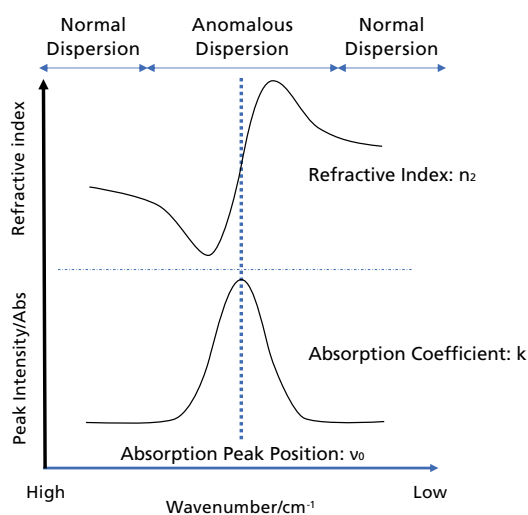


Fig. 1 Normal Dispersion and Anomalous Dispersion

The absorption coefficient varies symmetrically around the absorption peak position  $\nu_0$ , but the refractive index does not vary symmetrically. Normally, refractive index decreases monotonically with increasing wavelength (lower wavenumber) (normal dispersion) and increases sharply near the absorption peak position (anomalous dispersion). The magnitude of this change in refractive index causes the peak shape to become non-symmetrical when measured by the transmission method and other methods, and causes so-called distortion or a distorted peak shape. In the reference literature, anomalous dispersion is described as “a small refractive index on the high wavenumber side near the absorption band and a large refractive index on the low wavenumber side near the absorption band.”<sup>[1]</sup>

### (2) Measurement Techniques

When using the pellet method, the particle size of the sample can affect peak strength even at the same sample concentration. The reference literature states “poor spectra may result from inadequate grinding and large particle sizes.”<sup>[1]</sup> Mixing powder samples that have large-sized particles with KBr or Nujol can also produce peaks with significant distortion, sometimes described as the Christiansen effect. This distortion is also explained by differences in refractive index.<sup>[2]</sup>

This section shows spectra of calcite/calcium carbonate ( $\text{CaCO}_3$ ) obtained by the microscope transmission method, diffuse reflectance spectroscopy (DRS), the specular reflection method (SRM), and attenuated total reflection (ATR), and presents instructions and useful notes for each sampling technique.

#### 1. Microscope Transmission Method

For the microscope transmission method, the sample is prepared by compressing and flattening it between two diamond windows in a diamond cell. With this sampling technique the sample is not mixed with KBr, and measurements may be affected by the refractive index when there is strong absorption and a thick sample. A spectrum obtained by the microscope transmission method is shown in Fig. 2.

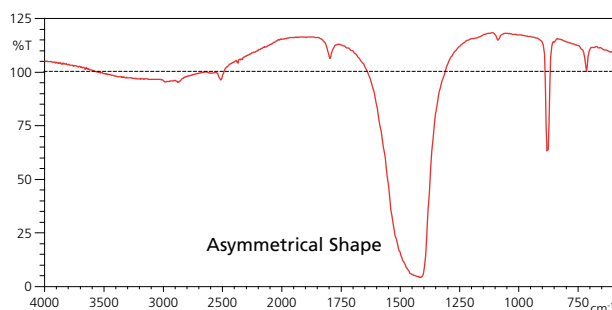


Fig. 2 Infrared Spectrum of Calcium Carbonate (Microscope Transmission Method)

In Fig. 2, the peak near  $1,400 \text{ cm}^{-1}$  shows strong absorption, indicating an asymmetrical shape due to the effects of anomalous dispersion as presented in Fig. 1.

In this case, measurements were taken using a diamond cell and diamond windows with a high refractive index. Because the layer of contact between the sample and diamond window is very thin, and the sample and diamond window have different refractive indices, reflectance at the interface is lower than that of diamond alone. This difference in reflective indices increases the transmittance of sample measurements compared with background measurements, causing the baseline position to be over 100 %. Using KBr as window material reduces the baseline to close to 100 % due to the low refractive index of KBr.

## 2. Diffuse Reflectance Spectroscopy

A spectrum obtained by diffuse reflectance spectroscopy is shown in Fig. 3.

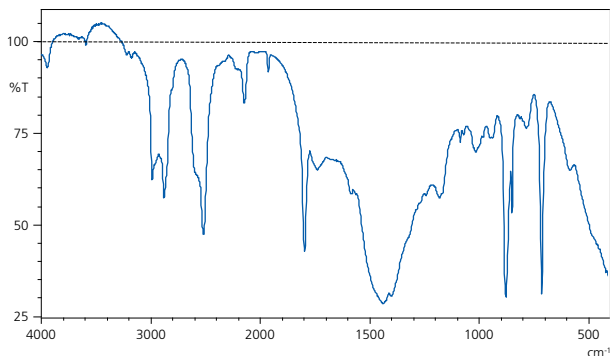


Fig. 3 Infrared Spectrum of Calcium Carbonate (Diffuse Reflectance Spectroscopy)

Like the KBr pellet method, in the diffuse reflectance spectroscopy method the sample is diluted with KBr, hence the distortion described above may also occur during diffuse reflectance spectroscopy when sample particles are not ground sufficiently small. Like transmission measurements, the baseline can also exceed 100 % when the KBr powder used for background measurements has a large particle size. Weaker absorption peaks are more enhanced in spectra obtained by diffuse reflectance spectroscopy than in spectra obtained by transmission measurements. This phenomenon occurs due to repeated transmission and reflection of infrared light inside the sample, which prevents the establishment of a proportional relationship between concentration and peak intensity expressed as absorbance. For this reason, when comparing diffuse reflectance spectroscopy spectra with transmission spectra or when using diffuse reflectance spectroscopy for quantitative analysis, scattering correction must be applied based on the K-M function as proposed by Kubelka and Munk.

## 3. Specular Reflection Method

A spectrum obtained by the specular reflection method is shown in Fig. 4.

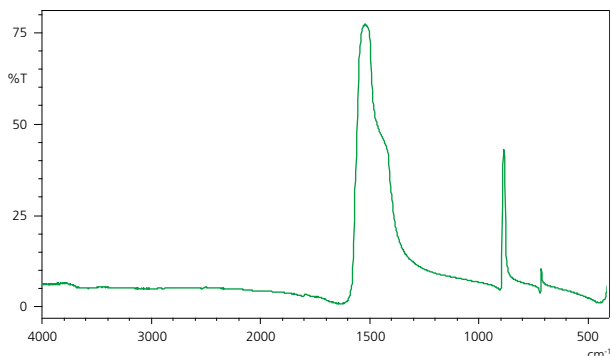


Fig. 4 Infrared Spectrum of Calcium Carbonate (Specular Reflection Method)

The specular reflection method creates a spectrum that is more influenced by refractive index than by absorption. Normally, specular reflection spectroscopy produces so-called derivative-shaped peaks that are mainly influenced by refractive index. Near a high absorption band, reflectance decreases from the high wavenumber side and increases significantly near the peak position. For this reason, as in Fig. 4, spectra obtained by the specular reflection method look as if it shows absorbance.

## 4. ATR Method

The ATR method is a technique for acquiring spectra that places the sample in close contact with the surface of a prism of an infrared transmitting material of high refractive index. The ATR method requires total reflection at the interface between the prism and sample, but reflectance decreases according to the intensity of absorption in the region of absorption by the sample. Therefore, although the ATR method produces spectra that appear to resemble the absorption spectra of transmission spectroscopy and other methods, caution is required as the spectra have different peak shapes and peak intensity ratios.<sup>[3,4]</sup>

In recent years, diamond has been one of the most common prism materials. Being the hardest material known to man, diamond prisms can be used with little concern for damage or scratching of the prism due to contact with the sample. A spectrum obtained by the ATR method using a diamond prism is shown in Fig. 5.

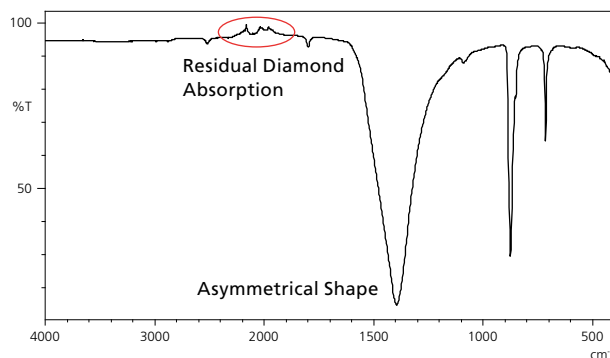


Fig. 5 Infrared Spectrum of Calcium Carbonate (ATR Method)

In Fig. 5, the peak near 1,400 cm⁻¹ is asymmetrical with broadening on the low wavenumber side.

The absorption bands in the opposite direction between 2,300 and 1,900 cm⁻¹ are caused by residual absorption from the diamond prism.

### 3. Peak Distortion in ATR Spectra

This section focuses solely on the ATR method and discusses peak distortion in more detail.

As mentioned earlier, when using the ATR method, reflectance decreases according to the intensity of absorption in the wavenumber region where there is absorption by the sample. Therefore, the degree of change in the refractive index of the sample is revealed in the spectrum as peak shift and peak distortion. Looking at Fig. 1, anomalous dispersion causes the refractive index to decrease on the high wavenumber side of the absorption peak. With the ATR method, a smaller refractive index is associated with a shallower depth of light penetration, which is revealed as increased reflectance in an ATR spectrum. This effect is explained later in this article using different data. Conversely, refractive index increases on the low wavenumber side of the absorption peak as shown in Fig. 1, thereby increasing the depth of light penetration. As the refractive index increases, the depth of light penetration increases and the peak intensity in the ATR spectrum increases. Thus, the peak position in the ATR spectrum is shifted more to the low wavenumber side compared with the absorption peak position  $\nu_0$  using the transmission method. This effect is explained below using ATR measurements from calcium carbonate.

One option for preventing peak shift and peak distortion is to use a prism with a high refractive index that will reduce the effect of the change in refractive index caused by anomalous dispersion. Germanium prisms (Ge, refractive index: 4.0) have the highest refractive index of all commercially available prisms. This high refractive index reduces the depth of light penetration, thereby reducing absorption band strength and reducing distortion.

Another option is to increase the angle of incidence, which reduces the depth of light penetration even using prisms made of diamond or zinc selenide (ZnSe) with a low refractive index. The effect is similar to that of using a Ge prism and is explained based on the relationship between total reflection and the sample and prism.<sup>[3]</sup>

Another effective option is to reduce the relative (apparent) refractive index, i.e., to weaken absorption, since strong absorption is also a factor in causing distortion. Kiyoshi Miyashita describes diluting the sample with matrix to reduce spectral distortion in his contribution to FTIR TALK LETTER Vol. 21 "The Information Available from Various FTIR Spectra and Avoiding Misinterpretation," also used as a resource for this article.

Here are presented some example ATR measurements of calcium carbonate and 2,3,4,5,6-pentabromotoluene (PBT) diluted with KBr.

#### (1) Peak Distortion with Calcium Carbonate

Fig. 6 shows spectra for calcium carbonate diluted with KBr at various dilution rates.

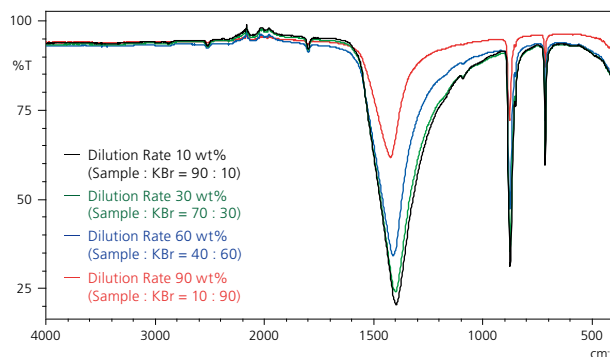


Fig. 6 Infrared Spectra of Calcium Carbonate Diluted with KBr (ATR Method)

Furthermore, Fig. 7 shows a magnified view of the wavenumber range 1,600 to 1,100  $\text{cm}^{-1}$  in Fig. 6.

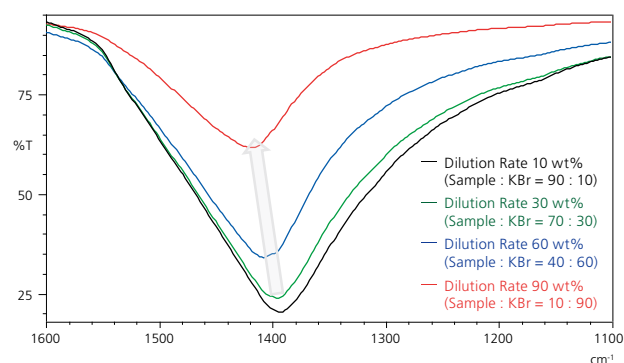


Fig. 7 Magnified View of the Wavenumber Range 1,600 to 1,100  $\text{cm}^{-1}$  in Fig. 6

Fig. 7 shows that the peak position near 1,400  $\text{cm}^{-1}$  shifts to a higher wavenumber with increasing dilution rate, i.e., it is close to the peak position seen in the transmission method spectrum. For more information on this topic, refer to Shimadzu's Application News No.A476 "Introduction of Advanced ATR Correction to Convert ATR Spectrum into Transmission Spectrum."

## (2) Peak Distortion with PBT

Similar measurements were performed with PBT, which has a high refractive index similar to calcium carbonate. PBT is a white to light brown powder or crystalline powder and is used as a brominated flame retardant in polymers.

Fig. 8 shows spectra for PBT diluted with KBr at various dilution rates.

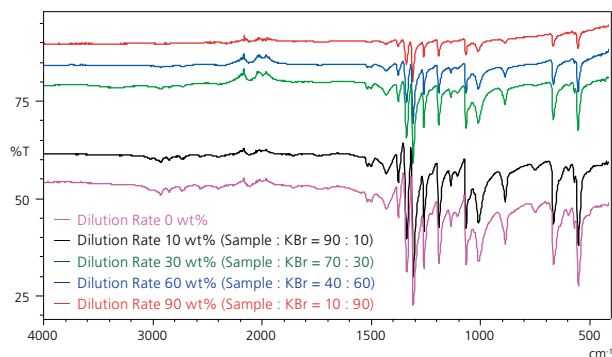


Fig. 8 Infrared Spectra of PBT Diluted with KBr (ATR Method)

Furthermore, Fig. 9 shows a magnified view of the wavenumber range 1,400 to 1,200  $\text{cm}^{-1}$  in Fig. 8. The baselines of the spectra in Fig. 9 have been aligned at 1,200  $\text{cm}^{-1}$ .

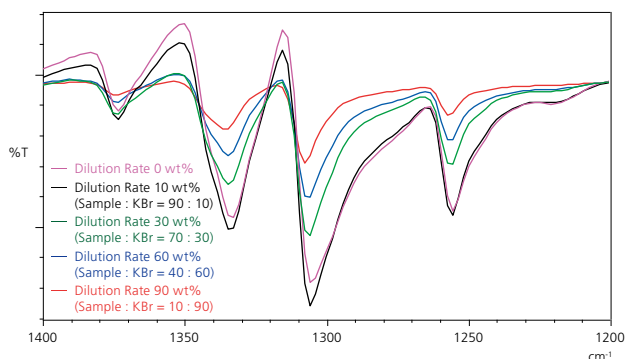


Fig. 9 Magnified View of the Wavenumber Range 1,400 to 1,200  $\text{cm}^{-1}$  in Fig. 8 (Baselines aligned at 1,200  $\text{cm}^{-1}$ )

Fig. 8 shows that due to the very high refractive index of PBT, the baseline (total reflectance) is positioned lower at lower dilution rates. Also, for peaks in the region 1,400 to 1,200  $\text{cm}^{-1}$ , Fig. 9 shows the lower the dilution rate, the more rapidly the baseline rises from the high wavenumber side as it approaches the peak position. As mentioned earlier, this distortion is thought to be caused by a smaller refractive index, shallower depth of light penetration, and resulting in higher reflectance on the high wavenumber side of the absorption peak position. Conversely, light penetrates deeper on the low wavenumber side of the absorption peak position, resulting in a broadening of the peak shape and peak distortion.

As described above, diluting the sample with KBr for ATR

measurements can reduce distortion for peaks showing strong absorption due to a high refractive index.

Apart from PBT presented here, other materials with a high refractive index that cause peak distortion include the sulfur-containing compound polyphenylene sulfide (PPS).<sup>[5,8]</sup> Similarly, peak distortion due to anomalous dispersion of the refractive index may occur with black rubber that contains carbon and has a high refractive index. For more information, see FTIR TALK LETTER Vol. 11, "Points to Note in Rubber Analysis: Black Rubber."

## 4. Conclusion

This article explained good spectra and the distortion found in spectra measured by various sampling techniques.

Depending on the sampling technique, peak shift and peak distortion can occur in the spectra of strongly absorbing samples such as calcium carbonate and the spectra of high refractive index samples such as PBT (both presented here). Whether peak shift and peak distortion originate from the sample or the sampling technique can be investigated when using the transmission method by varying parameters such as matrix particle size and concentration, and by varying prism material, angle of incidence, and concentration when using the ATR method.

We hope this article will prove useful in obtaining "good spectra."

## Acknowledgments

Finally, we would like to thank Yusuke Ishigaki of the Laboratory of Organic Chemistry I, Department of Chemistry, Faculty of Science, Hokkaido University for his advice on ATR measurements with KBr dilution.

## References

- [1] S. Tanaka, N. Teramae. *Infrared Spectroscopy: Experts Series for Analytical Chemistry Instrumentation Analysis*. Kyoritsu Shuppan (1993)
- [2] S. Tanaka. *Infrared and Raman Analysis. Basic Analytical Chemistry Course*. Kyoritsu Shuppan (1974)
- [3] K. Nishikida, R. Iwamoto. *Infrared Methods of Material Analysis*. Kodansha Scientific (1986)
- [4] T. Hasegawa, Y. Osaki. *Infrared and Raman Spectroscopy: Experts Series for Analytical Chemistry Instrumentation Analysis*. Kyoritsu Shuppan (2020)
- [5] S. Takayama. *How to Read Infrared Absorption Spectra of Polymers and Additives*. Science & Technology Presentation Materials (2018)
- [6] The Japan Society for Analytical Chemistry, Research Committee of Polymer Analysis, *Polymer Analysis Handbook*. Kinokuniya Shoten (1995)

## Q&A

# Do All ATR Spectra Require ATR Correction?

ATR correction modifies infrared spectra acquired by the ATR method to approximate a transmission spectrum. Spectra acquired by the ATR method are known to have different peak intensity ratios and peak positions compared with transmission spectra, and are also affected by polarization characteristics.

There is no need to apply ATR correction when comparing only ATR spectra. An increasing number of libraries now contain ATR spectra, and these ATR spectra can be compared without correction.

However, when comparing ATR spectra with transmission spectra, ATR correction must be applied for more accurate results.

Shimadzu's advanced ATR correction simultaneously corrects for three factors: peak intensity, peak position, and polarization characteristics.

Fig. 1 shows the ATR spectrum and transmission spectrum of a polycarbonate. As can be observed, not only the peak intensities but also the peak positions are very different. Fig. 2 shows the spectrum obtained by applying advanced ATR correction to the ATR spectrum shown in Fig. 1. Advanced ATR correction largely eliminates the disparities between the ATR spectrum and transmission spectrum. For more information on this topic, refer to Shimadzu's Application News No. A476.

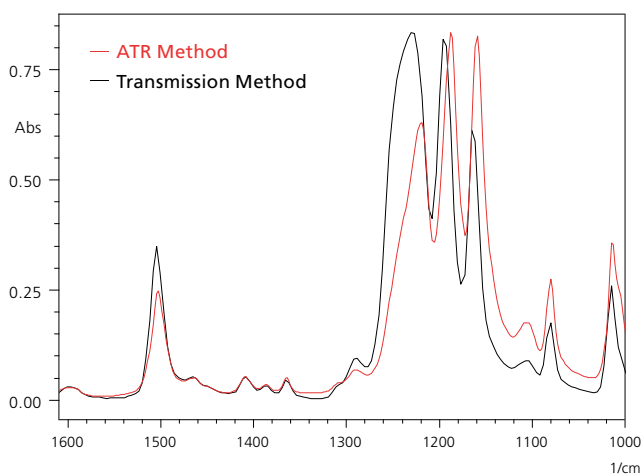


Fig. 1 ATR Spectrum and Transmission Spectrum

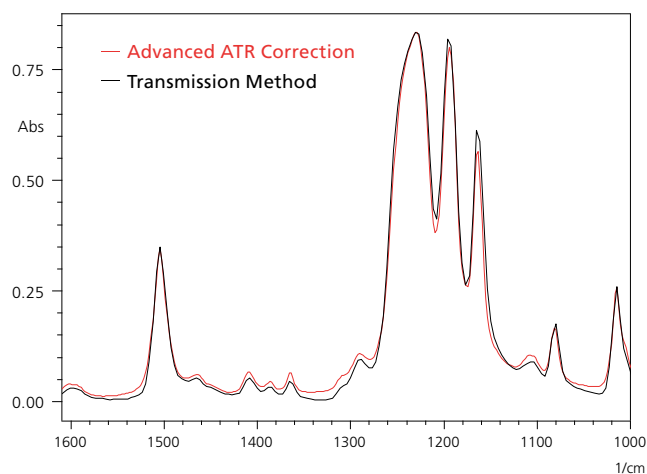


Fig. 2 After Applying Advanced ATR Correction

Fourier Transform Infrared Spectrophotometer

# IRXross



## IR, Xross over

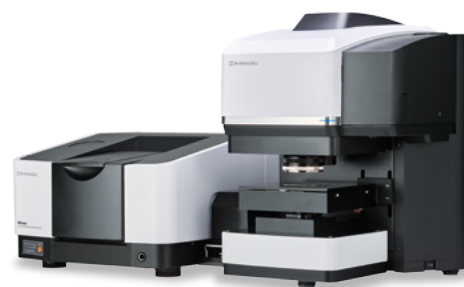
Performance × Operability

The IRXross™ creates a new concept for infrared spectroscopy. It offers the optimal solution for a new era with diverse application requirements.

**High-End Sensitivity for  
Countless Applications**

**Built-in Analytical Intelligence**

**Complies Fully with Regulations**



Infrared Microscope System



Shimadzu Corporation  
[www.shimadzu.com/an/](http://www.shimadzu.com/an/)

**For Research Use Only. Not for use in diagnostic procedures.**

This publication may contain references to products that are not available in your country. Please contact us to check the availability of these products in your country.

Company names, products/service names and logos used in this publication are trademarks and trade names of Shimadzu Corporation, its subsidiaries or its affiliates, whether or not they are used with trademark symbol "TM" or "®".

Third-party trademarks and trade names may be used in this publication to refer to either the entities or their products/services, whether or not they are used with trademark symbol "TM" or "®".

Shimadzu disclaims any proprietary interest in trademarks and trade names other than its own.

The contents of this publication are provided to you "as is" without warranty of any kind, and are subject to change without notice. Shimadzu does not assume any responsibility or liability for any damage, whether direct or indirect, relating to the use of this publication.